Clinical utility of three-dimensional magnetic resonance imaging using a zero-echo-time sequence in endoscopic endonasal transsphenoidal surgery

Akihiro Inoue (iakihiro3@gmail.com)
Ehime university school of medicine https://orcid.org/0000-0002-7438-2369
Shohei Kohno
Himeji Sekijuji Byoin
Naoya Nishida
Ehime Daigaku Daigakuin Igakukei Kenkyuka Igakubu
Satoshi Suehiro
Ehime Daigaku Daigakuin Igakukei Kenkyuka Igakubu
Shirabe Matsumoto
Ehime Daigaku Daigakuin Igakukei Kenkyuka Igakubu
Masahiro Nishikawa
Ehime Daigaku Daigakuin Igakukei Kenkyuka Igakubu
Saya Ozaki
Ehime Daigaku Daigakuin Igakukei Kenkyuka Igakubu
Yawara Nakamura
Ehime Daigaku Daigakuin Igakukei Kenkyuka Igakubu
Seiji Shigekawa
Ehime Daigaku Daigakuin Igakukei Kenkyuka Igakubu
Hideaki Watanabe
Ehime Daigaku Daigakuin Igakukei Kenkyuka Igakubu
Hidenori Senba
Ehime Daigaku Daigakuin Igakukei Kenkyuka Igakubu
Bunzo Matsuura
Ehime Daigaku Daigakuin Igakukei Kenkyuka Igakubu
Takeharu Kunieda
Ehime Daigaku Daigakuin Igakukei Kenkyuka Igakubu

Research article

Keywords: zero-echo-time sequence-based magnetic resonance imaging, magnetic resonance angiography, endoscopic transsphenoidal surgery, new three-dimensional modeling, pituitary tumor

DOI: https://doi.org/10.21203/rs.2.15421/v1

Abstract

Background: Recognizing the anatomical orientation surrounding the sellar floor is crucial in endoscopic endonasal transsphenoidal surgery (ETSS). Zero-echo-time (ZTE) sequences were recently suggested for a new bone identification technique on magnetic resonance imaging (MRI). This study aimed to evaluate the clinical usefulness of three-dimensional (3D)-ZTE-based MRI models in providing anatomical guidance for ETSS.

Methods: ZTE-based MRI and magnetic resonance angiography (MRA) data from 15 consecutive patients with pituitary tumor treated between September 2018 and May 2019 were used to create 3D-MRI models. From these, the architecture surrounding the sellar floor, particularly anatomical relationships between tumors and internal carotid arteries (ICAs), was visualized to preoperatively plan surgical procedures. In addition, 3D-ZTE-based MRI models were compared to actual surgical views during ETSS to evaluate model applicability.

Results: These 3D-ZTE-based MRI models clearly demonstrated the morphology of the sellar floor and matched well with intraoperative views, including pituitary tumor, by successively eliminating sphenoidal structures. The models also permitted determination of the maximum marginal line of the opening of the sellar floor by presenting vital structures such as ICAs and tumors. With such 3D-MRI models, the surgeon could access the intracranial area through the sellar floor more safely, and resect the pituitary tumor maximally without complications.

Conclusions: Our 3D-MRI models based on ZTE sequences allowed distinct visualization of vital structures and pituitary tumor around the sellar floor. This new method using 3D-ZTE-based MRI models showed low invasiveness for patients and was useful in preoperative planning for ETSS, facilitating maximum tumor resection without complications.

Background

Endoscopic endonasal transsphenoidal surgery (ETSS) has become increasingly used to access pituitary tumors and other midline skull-based lesions [1, 2]. There are several technical advantages to ETSS, such as wider, multidirectional views of the operative field. Nevertheless, there is a significant risk that surrounding vital structures could be injured, particularly when there is extensive tumor invasion into the sphenoid sinus and involvement of the internal carotid arteries (ICAs) [3]. In such cases, it is important to accurately identify the positional relationships of vital structures preoperatively, especially when the surgeon lacks complete familiarity with the surgical field of ETSS. We have proposed the usefulness of three-dimensional (3D)-computed tomography (CT)-based models or reconstructed 3D-CT/magnetic resonance imaging (MRI) fusion models for obtaining preoperative orientation and providing a road map to ETSS *(Fig. 1A, B)* [4, 5]. However, major obstacles exist to acquiring CT images for creating these 3D models, such as excessive radiation exposure and the necessity for administration of iodocontrast media to depict bilateral ICAs. Recently, zero-echo-time (ZTE)-based segmentation methods on MRI have been

suggested as a new bone-identification technique [6–9]. ZTE was designed to achieve signals from cortical bone for tissue segmentation, and as such can be used to incorporate the bone in MR-based attenuation correction [6–9]. In addition, magnetic resonance angiography (MRA) techniques have improved markedly and we have been able to easily and clearly evaluate the vasculature without using iodocontrast medium [10]. We therefore created new 3D-MRI models combining ZTE-based MRI to depict the bone of the skull base and MRA to visualize ICAs, which can demonstrate the positional relationship between the pituitary tumor and surrounding sellar structures *(Fig. 1C).* The present study describes details of this reconstruction process, and reports that our 3D-ZTE-based MRI models show low invasiveness for patients, and high utility in obtaining preoperative orientation regarding vital structures of the sphenoid sinus and providing a road map to ETSS.

Methods

All procedures performed in studies involving human participants were in accordance with the ethical standards of the institutional and/or national research committee and with the 1964 Declaration of Helsinki and its later amendments or comparable ethical standards. The present study was approved by the local ethics committee for clinical research.

Experimental design

In this study, MRI was performed for 15 consecutive cases of endoscopic endonasal transsphenoidal pituitary surgery for pituitary tumor in our hospital between September 2018 and May 2019 *(Table 1).* The 3D-MRI-based models were created by the radiologist (Taichi Furumochi) before surgery for each patient. All patients were operated on using these 3D-MRI models in addition to the navigation system (StealthStation®; Medtronic, Minneapolis, MN) and an indocyanine green (ICG) endoscope (Karl Storz, Tuttlingen). Details of these methods are described in the paragraphs that follow. Informed consent was obtained from all individual participants enrolled in the study, including for the surgical procedure and potential risks of ETSS.

Constructed 3D-ZTE based MRI models.

MRI and MRA were performed before surgery using a 3.0-T whole-body MR scanner (General Electric (GE) Healthcare, Waukesha, WI) and an eight-channel phased-array head coil. For each patient, a high-resolution anatomic data set was scanned using 3D spoiled gradient recalled echo sequences (repetition time (TR), 15 ms; echo time (TE), 2.3 ms; flip angle, 10; matrix, 256 × 320; field of view (FOV), 230 mm; thickness, 0.9 mm) with gadopentetate dimeglumine. Data on ICAs was scanned using 3D time-of-flight MRA (3D-TOF-MRA) sequences (TR, 23 ms; TE, 3.4 ms; flip angle, 18; matrix, 416 × 224; FOV, 230 mm; thickness; 0.5 mm). In addition, the present study adopted a new bone imaging paradigm based on proton density (PD)-weighted ZTE. This sequence is based on a 3D gradient-echo imaging technique with a very short TE and low flip angles. The inherent contrast without any preparatory pulses is similar to proton density. The pulse sequence uses a 3D radial center-out sampling scheme where endpoints of

each spoke follow a spiral path in time. Isotropic voxels are acquired with TE close to 0 ms. The acquisition lasted 393 s, covering a 12-cm transaxial and 26-cm axial field of view with a resolution of 1.0 1.0 1.0 mm. Four excitations were acquired, with a flip angle of 1°and 62.5-kHz bandwidth.

A 3D Advantage Workstation Volume Share 4 (GE Healthcare) was used to process the acquired MRI data, according to our previous reports [4, 5]. Step 1 involves rendering volume and defining opacity −250 to +600 as the skin parameter. Step 2 involves setting the FOV to 18 cm and adjusting the pituitary gland to be in the center of the monitor with other images (either axial, coronal, or sagittal). Step 3 involves setting the position and selecting the volume-rendering Front Cut function (squarely whittling at the image), and then cutting from the tip of the nose to the end of the virus ring. Step 4 involves confirming the position and scope, and then saving. In Step 5, the ZTE MRI volume-rendered (VR) image resulting from the above process is overlaid onto the MRA image and the VR image obtained from contrast-enhanced MRI. Step 6 involves overlaying the image, performing (1) autofusion (overlaying an image with automatic adjustment of FOV and position information) or (2) manual fusion (overlaying an image while checking the image and adjusting the triaxial X-Y-Z). Step 7 involves confirming the fusion image and saving. The Digital Imaging and Communications in Medicine (DICOM) format was used to store the acquired fusion image model data from MRI. Digital snapshots taken at different phases of the simulated operation were used to prepare a slide presentation file, which was then used as a visual reference during the actual surgery. Based on the 3D model images, the locations of the tumor and vital structures, including the bony prominences of the ICAs buried under the invasive tumor were evaluated and compared with the actual intraoperative endoscopic views.

Statistical methods

Statistical analysis was performed using Fisher's exact test for categorical variables and analysis of variance for continuous variables. Two-tailed tests were performed for each scenario, and the significance level was set at $P < 0.05$. All analyses were performed using Office Excel 2016 software (Microsoft, Redmond, WA).

Results

The underlying pathology in the 15 patients included in the present study was pituitary adenomas (n = 9), craniopharyngioma (n = 2) or Rathke's cleft cyst (n = 4) *(Table 1).* The hormonal types of the pituitary adenomas were nonfunctioning macroadenoma (n = 6), growth hormone-producing microadenoma (n = 2), and prolactin (PRL)-producing microadenoma (n = 1). Mean age at the time of surgery was 55.9 years (range, 24–80 years). Subjects comprised 8 females (53.3%) and 7 males (46.7%). No significant difference in age was evident between male and female patients ($P > 0.05$). All 15 patients underwent ETSS using a neuro-navigation system and ICG endoscope assistance.

We were able to obtain ZTE-based MRI data (proton density image) for all patients *(Fig. 2A).* After acquiring the proton density images, we converted these data into CT-like ZTE images to be able to recognize bone *(Fig. 2B).* In all patients, CT-like bone depiction was identified clearly surrounding the

sellar floor in the sphenoid sinus *(Fig. 3).* In addition, we successfully created 3D-MRI models by combining these ZTE-based MRI data set and acquired MRA images *(Figs. 1C, 4, 5).* In these models, critical structures such as the ICAs, sellar floor and pituitary tumor were completely reconstructed, and spatial relationships were better visualized by successively deleting images of adjacent bony structure, even if ICAs were involved in the tumor. Furthermore, we clearly recognized the positional relationship between the ICAs and invasive tumor. The 3D-MRI model was able to be viewed in the operating room during surgery as multislice presentations on a computer monitor. Compared to existing 3D-CT-based models or 3D-CT/MRI fusion models, no inferiority was encountered in grasping the anatomical positions surrounding the sellar floor for anatomical guidance in ETSS *(Fig. 1),* and this reconstruction model had the advantage of needing no radiation exposure or iodine contrast agent.

Illustrative cases

Case 1

An 80-year-old man complained of headache and deterioration of visual function. Gadolinium (Gd)-enhanced MRI showed a macroadenoma invading into the right cavernous sinus (Knops classification: grade 3) *(Fig. 4A, B).* A preoperative 3D-ZTE-based MRI model demonstrated anatomical landmarks within the sphenoid sinus, including bony prominences of the ICAs and pituitary tumor*(Fig. 4C).* Under the guidance of this 3D-MRI model, we made a preoperative plan for the extent of opening of the sella and carried out ETSS, with modeled images appearing almost the same as the actual intraoperative views *(Fig. 4D).* In addition, the ICG endoscope allowed visualization of the bilateral ICAs 10 s after ICG flushing in accordance with 3D-MRI model *(Fig. 4E).* The tumor was totally removed without any complications and the patient showed full recovery of visual acuity and fields.

Case 2

A 52-year-old woman visited our department after demonstrating gradually worsening visual field deficits. Laboratory studies showed a high plasma level of PRL (74.7 pg/ml). Coronal and sagittal Gd-enhanced MRI showed a macroadenoma involving bilateral ICAs with invasion into the sphenoid sinus and destruction of the sellar floor *(Fig. 5A, B).* A preoperative 3D-ZTE-based MRI model clearly revealed the location of bilateral ICAs by successively eliminating bony structures *(Fig. 5D),* and we identified the exact location of ICAs buried in the tumor *(Fig. 5C).* As a result, we safely achieved maximum resection of the tumor without injuring the ICAs.

Discussion

ETSS has been found to be highly effective for resecting pituitary tumors with supra- and/or infrasellar extension, including lesions of the midline skull base [1, 2]. However, the disadvantage of this approach is that, with wide opening of the sellar floor, there is a risk that the surgeon may come extremely close to the ICA. To avoid ICA injury, a 3D-CT-based model or a 3D-CT/MRI fusion model that helps clarify the

anatomy of the nasal cavity and paranasal sinuses has been proposed and adopted [4, 5]. These models provide clearer orientation to the surgeon, which is critical when performing ETSS. Furthermore, preoperative surgical planning can be performed with optimization of these models according to the individual patient's anatomy [4, 5]. However, creation of both of these 3D-CT-based models and 3D-CT/MRI fusion models also has several disadvantages, including excessive radiation exposure for patients from CT and the need to use iodine contrast agents to visualize the ICA.

Generally, MRI is a noninvasive and essential diagnostic technique because of its inherent advantage of obtaining excellent soft-tissue contrast and high resolution of anatomical detail in the body without radiation exposure [9, 11]. However, this modality is considered inappropriate for depicting cortical bone structures because of the low proton density and very short T2 relaxation time [9, 12]. The current gold standard imaging technique to reveal bone structures is CT. However, a new bone identification technique has recently been published, based on 3D radial ZTE imaging on MRI [8, 13, 14]. In particular, GE Healthcare has developed an investigational work-in-progress (WIP) MR research package called ZTE for bone imaging, consisting of a pulse sequence technique designed to image cortical bone surfaces [3, 4]. The ZTE sequence is a 3D radial sequence used for silent MRI, and the extremely short effective TE allows detection of the shortest T2 tissues, including cortical bone [6, 9]. To date, such MR bone imaging using ZTE sequences has been applied to positron emission tomography (PET)/MRI attenuation correction from the perspective of the technical approach in the literature and clinical diagnostic use of osseous shoulder or skull bone imaging [6, 9, 13]. Above all, in neuroradiology, ZTE skull MRI has been gradually introduced to evaluate skull lesions in patients with head trauma [9]. This ZTE sequence has the advantage of being able to visualize bones without radiation exposure, unlike CT. On the other hand, several problems have been reported for ZTE sequences [6]. In previous reports, the boundary of bone and fluid as found in the inner ear was proposed to be a major problem for ZTE. Furthermore, accuracy was reported to be insufficient at the base of the skull bone or around the paranasal sinuses [6]. In particular, the mastoid air cells, despite also being complex anatomical structures, were found to pose fewer issues. In the present study, we applied the ZTE sequence to obtain images of the skull bones of patients with pituitary tumor. Certainly, according to previous reports, bone depiction using the ZTE sequence is inferior to that using CT imaging in the sense of clearly recognizing anatomical bone structures of the skull base around the sellar floor in our study. However, the ZTE sequence can play a sufficient role in identifying the positional relationship between ICAs and tumor compared to CT images, and in understanding the position of the tumor inside the sellar during ETSS. In fact, we performed ETSS safely using only ZTE-based MRI. MRA techniques have also improved markedly in recent years and we have been able to easily and clearly evaluate the vasculature on systemic MRA [10]. In particularly, when we identify the ICA position during ETSS, no difference is evident between MRA and CTA in the depiction of ICAs surrounding the sellar lesion. In addition, since MRA techniques do not require a contrast agent for vessel visualization, good vessel depiction can be achieved even in patients with poor renal function.

In this study, we created 3D-MRI models of surrounding sellar floor for the purpose of achieving safe operations on ETSS by combining ZTE-based MRI and MRA. As with our previously reported 3D-CT-based and 3D-CT/MRI fusion models, this 3D-ZTE-based MRI model provided surgeons with a clear anatomical

orientation, which is critical for performing ETSS. Furthermore, the model can be optimized for preoperative surgical planning according to the individual anatomy of the patient. In addition, the greatest advantage of this model seems to be the low invasiveness to patients. To the best of our knowledge, this represents the first clinical report of the usefulness of 3D models using ZTE-based MRI for the safety of skull base surgery, in particular ETSS. The present 3D modelling process requires further refinement, but our 3D models provide critical anatomical information for preoperatively determining strategy and for anatomical guidance according to which neurosurgeons can carry out transsphenoidal surgery more smoothly and safely.

Conclusions

Our new 3D models combining ZTE-based MRI and MRA enabled neurosurgeons to obtain an appropriate orientation of the surrounding sellar floor for ETSS similar to existing 3D-CT-based models and 3D-CT/MRI fusion models. Using this model, we obtained information on the exact locations of ICAs and anatomical relationships between the sellar floor and pituitary tumor. The models presented here are very useful as road maps for guiding actual surgical procedures and have the possibility to develop as a new assistant modality for ETSS.

Abbreviations

ETSS: Endoscopic endonasal transsphenoidal surgery; ICAs: internal carotid arteries; 3D: three-dimensional; CT: computed tomography; MRI: magnetic resonance imaging; ZTE: zero-echo-time; MRA: magnetic resonance angiography; ICG: indocyanine green; GE: General Electric; TR: repetition time; TE; echo time; FOV: field of view; TOF: time-of-flight; PD: proton density; VR: volume-rendered; DICOM: Digital Imaging and Communications in Medicine; Gd: Gadolinium; WIP: work-in-progress; PET: positron emission tomography

Declarations

Acknowledgements

The authors would like to express their gratitude to Taichi Furumochi and Yasuhiro Shiraishi of the Department of Neurology, Ehime University Hospital, Japan, for their helpful information regarding radiological image acquisition. In particular, Taichi Furumochi contributed extensively to the construction of 3D-MRI models in this research. We also thank Hiroyuki Kabasawa, Atsushi Nozaki, Kohei Miura, Koji Maehara at GE Healthcare Japan for their advice regarding the technical background of ZTE sequences and the postprocessing steps during the revision process.

Author’s contributions

All authors (AI, SK, NN, SS, SM, MN, SO, YN, SS, HW, HS, BM and TK) have made substantial contributions to acquisition of data, or analysis and interpretation of data. They have been involved in drafting the manuscript or revising it critically for important intellectual content. The authors have given final approval of the version to be published and agreed to be accountable for all aspects of the work in ensuring that questions related to the accuracy or integrity of any part of the work are appropriately investigated and resolved. Each author -namely SK, NN, SM, MN, HS and TK- has participated sufficiently in the work to take public responsibility for appropriate portions of the content.

Funding

This research did not receive any specific grant from funding agencies in the public, commercial, or not-for-profit sectors

Availability of data and materials

The datasets analysed during the current study are available from the corresponding author on reasonable request.

Ethics approval and consent to participate

All procedures performed in studies involving human participants were in accordance with the ethical standards of the institutional and/or national research committee and with the 1964 Declaration of Helsinki and its later amendments or comparable ethical standards. The present study was approved by the local ethics committee for clinical research. The clinical study of the following studies was approved by the Ethics Committee for Clinical Research of Ehime University Hospital prior to initiating the study. Informed consent was obtained from each patient prior to initiating the study.

Consent for publication

Not applicable.

Competing interests

The authors declare that they have no competing interests.

Author details

[1]Department of Neurosurgery, Ehime University School of Medicine 454 Shitsukawa, Toon, Ehime 791–0295, Japan. [2]Department of Neurosurgery, Japanese Red Cross Society Himeji Hospital 1–12–1 Shimoteno, Himeji, Hyogo 670–8540, Japan. [3]Department of Otolaryngology, Ehime University School of

Medicine, 454 Shitsukawa, Toon, Ehime 791–0295, Japan. [4]Department of Lifestyle-related Medicine and Endocrinology, Ehime University School of Medicine, 454 Shitsukawa, Toon, Ehime 791–0295, Japan.

References

[1] Jho HD, Alfieri A. Endoscopic endonasal pituitary surgery: evolution of surgical technique and equipment in 150 operations. Minim Invasive Neurosurg. 2001; 44 (1): 1–12.

[2] Frank G, Pasquini E, Farneti G, Mazzatenta D, Sciarretta V, Grasso V, Faustini Fustini M. The endoscopic versus the traditional approach in pituitary surgery. Neuroendocrinology. 2006; 83 (3–4): 240–8.

[3] Catapano D, Sloffer CA, Frank G, Pasquini E, D'Angelo VA, Lanzino G. Comparison between the microscope and endoscope in the direct endonasal extended transsphenoidal approach: anatomical study. J Neurosurg. 2006; 104 (3): 419–25.

[4] Inoue A, Ohnishi T, Kohno S, Harada H, Nishikawa M, Ozaki S, Matsumoto S, Ohue S. Utility of three-dimensional computed tomography for anatomical assistance in endoscopic endonasal transsphenoidal surgery. Neurosurg Rev. 2015; 38 (3): 559–65.

[5] Inoue A, Ohnishi T, Kohno S, Nishida N, Nakamura Y, Ohtsuka Y, Matsumoto S, Ohue S. Usefulness of an image fusion model using three-dimensional CT and MRI with indocyanine green fluorescence endoscopy as a multimodal assistant system in endoscopic transsphenoidal surgery. Int J Endocrinol. 2015: 694273.

[6] Delso G, Wiesinger F, Sacolick LI, Kaushik SS, Shanbhag DD, Hüllner M, Veit-Haibach P. Clinical evaluation of zero-echo-time MR imaging for the segmentation of the skull. J Nucl Med. 2015; 56 (3): 417–22.

[7] Sekine T, Ter Voert EE, Warnock G, Buck A, Huellner M, Veit-Haibach P, Delso G. Clinical evaluation of zero-echo-time attenuation correction for brain 18F-FDG PET/MRI: comparison with atlas attenuation correction. J Nucl Med. 2016; 57 (12): 1927–32.

[8] Wiesinger F, Sacolick LI, Menini A, Kaushik SS, Ahn S, Veit-Haibach P, Delso G, Shanbhag DD. Zero TE MR bone imaging in the head. Magn Reson Med. 2016; 75 (1): 107–14.

[9] Cho SB, Baek HJ, Ryu KH, Choi BH, Moon JI, Kim TB, Kim SK, Park H, Hwang MJ. Clinical feasibility of zero TE skull MRI in patients with head trauma in comparison with CT: a single-center study. AJNR Am J Neuroradiol. 2019; 40 (1): 109–15.

[10] Kuo PH, Kanal E, Abu-Alfa AK, Cowper SE. Gadolinium based MR contrast agents and nephrogenic systemic fibrosis. Radiology. 2007; 242 (3): 647–9.

[11] Blystad I, Warntjes JB, Smedby O, Landtblom AM, Lundberg P, Larsson EM. Synthetic MRI of the brain in a clinical setting. Acta Radiol. 2012; 53 (10): 1158–63.

[12] Du J, Carl M, Bydder M, Takahashi A, Chung CB, Bydder GM. Qualitative and quantitative ultrashort echo time (UTE) imaging of cortical bone. J Magn Reson. 2010; 207 (2): 304–11.

[13] Madio DP, Lowe IJ. Ultra-fast imaging using low flip angles and FIDs. Magn Reson Med. 1995; 34 (4): 525–9.

[14] Wu Y, Ackerman JL, Chesler DA, Graham L, Wang Y, Glimcher MJ. Density of organic matrix of native mineralized bone measured by water- and fat-suppressed proton projection MRI. Magn Reson Med. 2003; 50 (1): 59–68.

Tables

Due to technical limitations, tables are only available as a download in the supplemental files section

Figures

Fig. 1

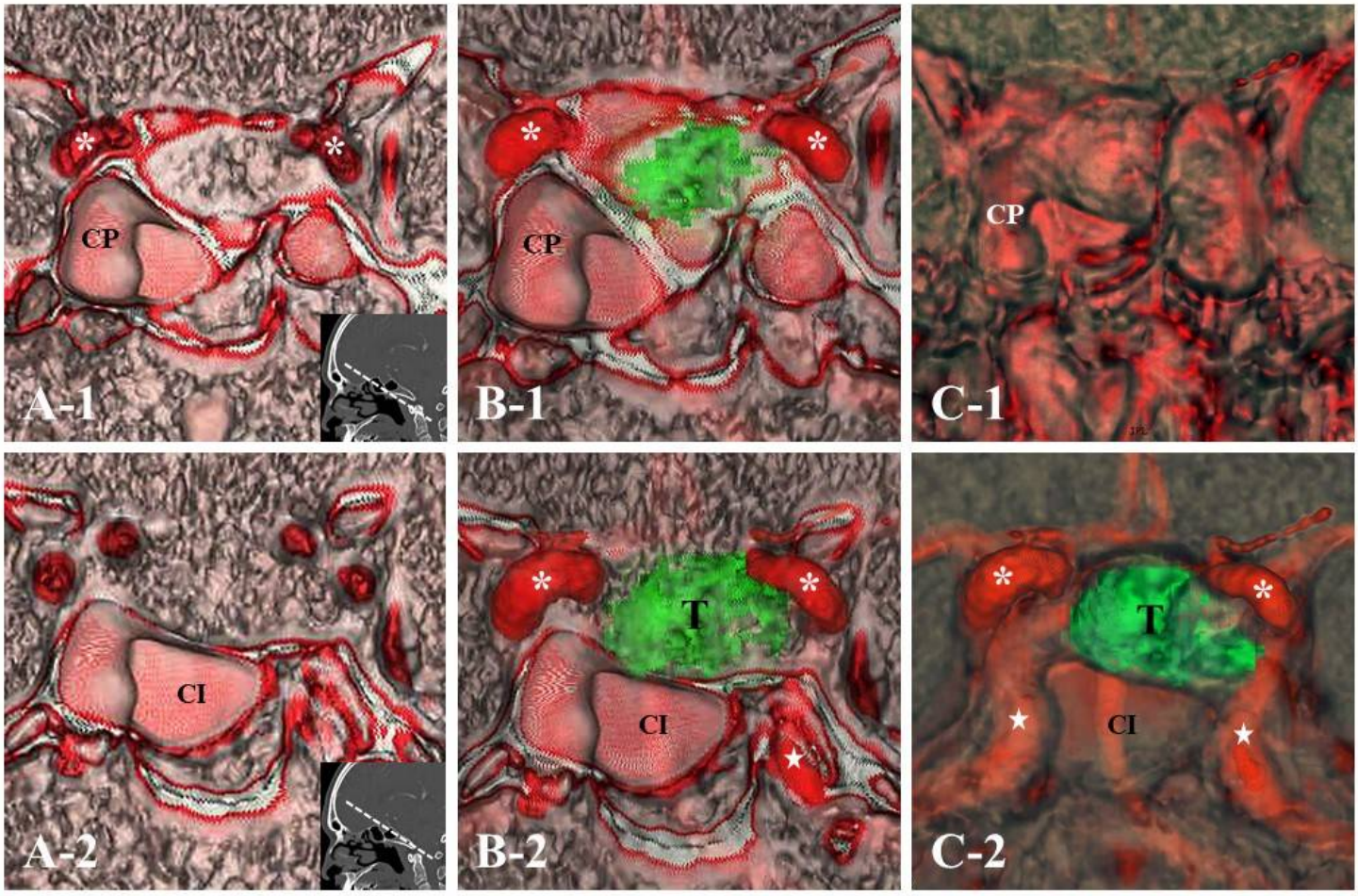

Figure 1

Simulated view of the endonasal transsphenoidal approach using a three-dimensional (3D) computed tomography (CT)-based model (A), 3D-CT/magnetic resonance imaging (MRI) fusion models (B) and 3D-zero-echo-time (ZTE)-based MRI model (C) showing tumor (green object) and bony prominences of the internal carotid arteries (ICAs) around the sellar floor (CI: clival indentation; CP: ICA prominence; white stars ICA: C4 portion, white asterisks: ICA C3 portion in cavernous sinus; T: tumor).

Fig. 2

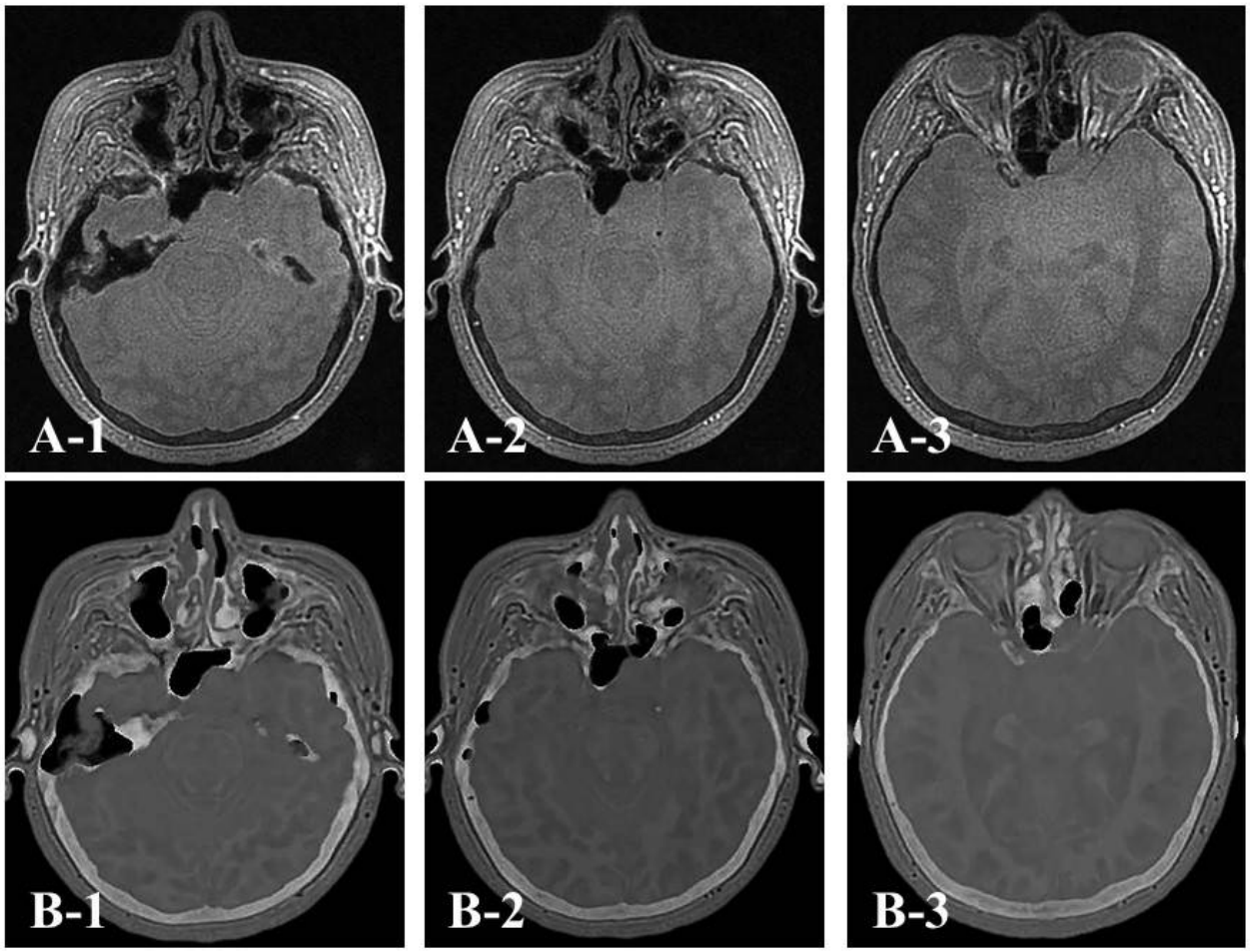

Figure 2

Axial views of a typical ZTE dataset for the skull base region. A) Axial proton-density images. B) Axial CT-like contrast ZTE images.

Fig. 3

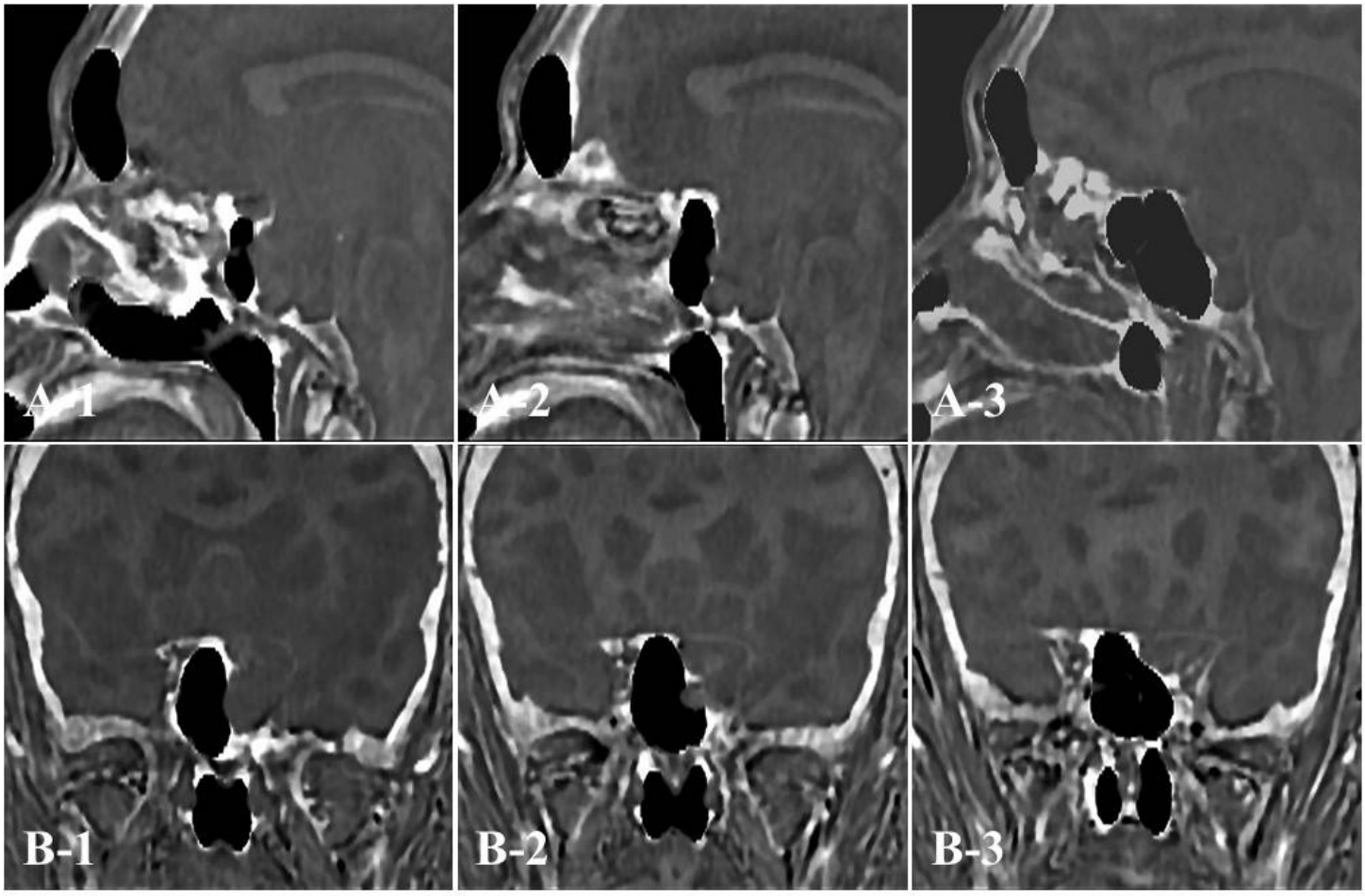

Figure 3

Sagittal (A) and coronal (B) CT-like ZTE images at the surrounding sellar floor. These images clearly show skull base bone around the sella turcica.

Fig. 4

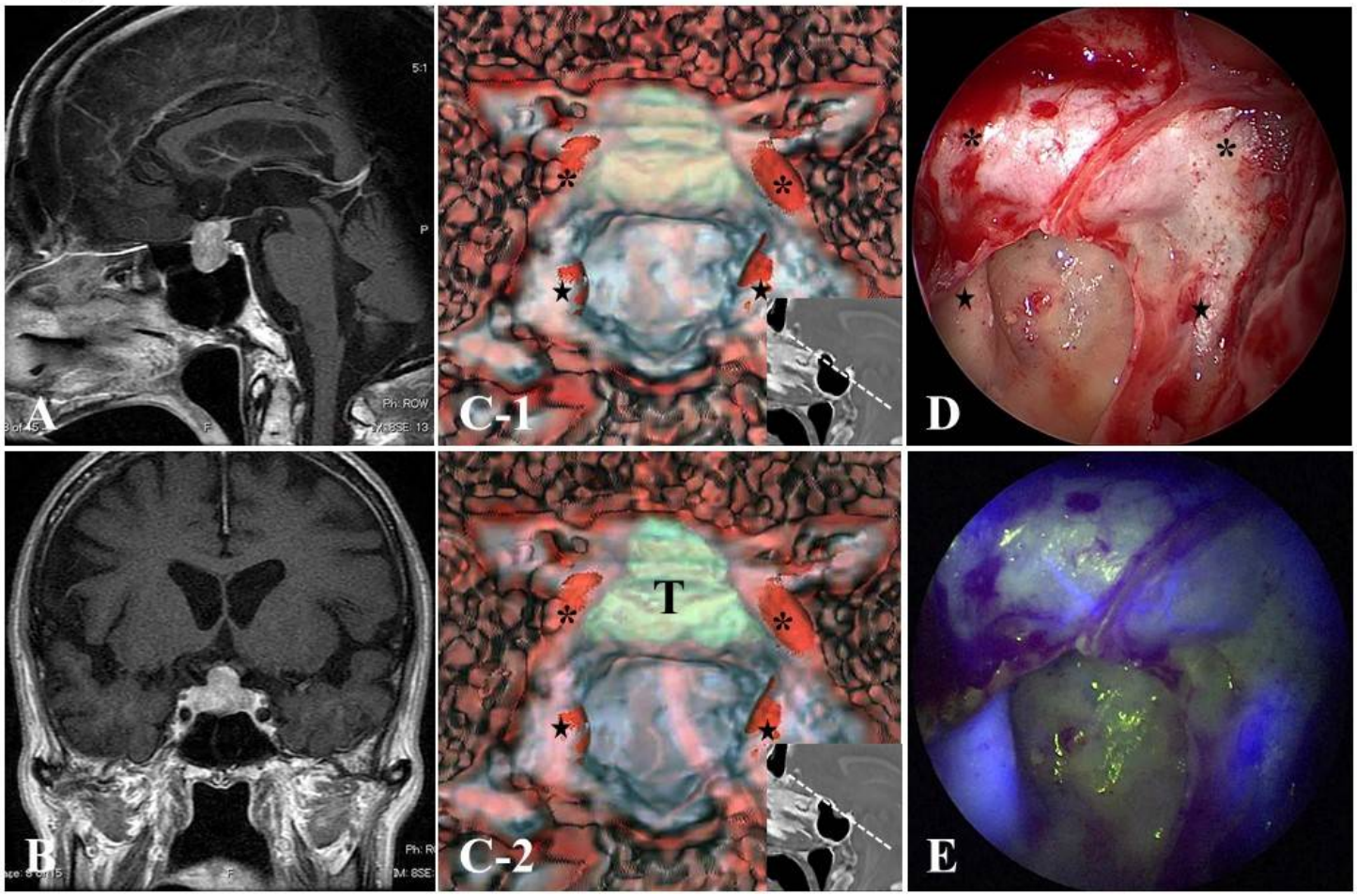

Figure 4

Preoperative sagittal and coronal Gd-enhanced MRI (A, B) in Case 1 show a pituitary tumor with suprasellar extension and right cavernous invasion. Preoperative 3D-ZTE-based MRI of the surrounding sellar floor (C) reveals bilateral ICAs (C3: black asterisk; C4: black star) and pituitary tumor (T: green object) matching well with intraoperative endoscopic views (D) (C3: black asterisk; C4: black star) and indocyanine green (ICG) endoscope views (E). T, tumor.

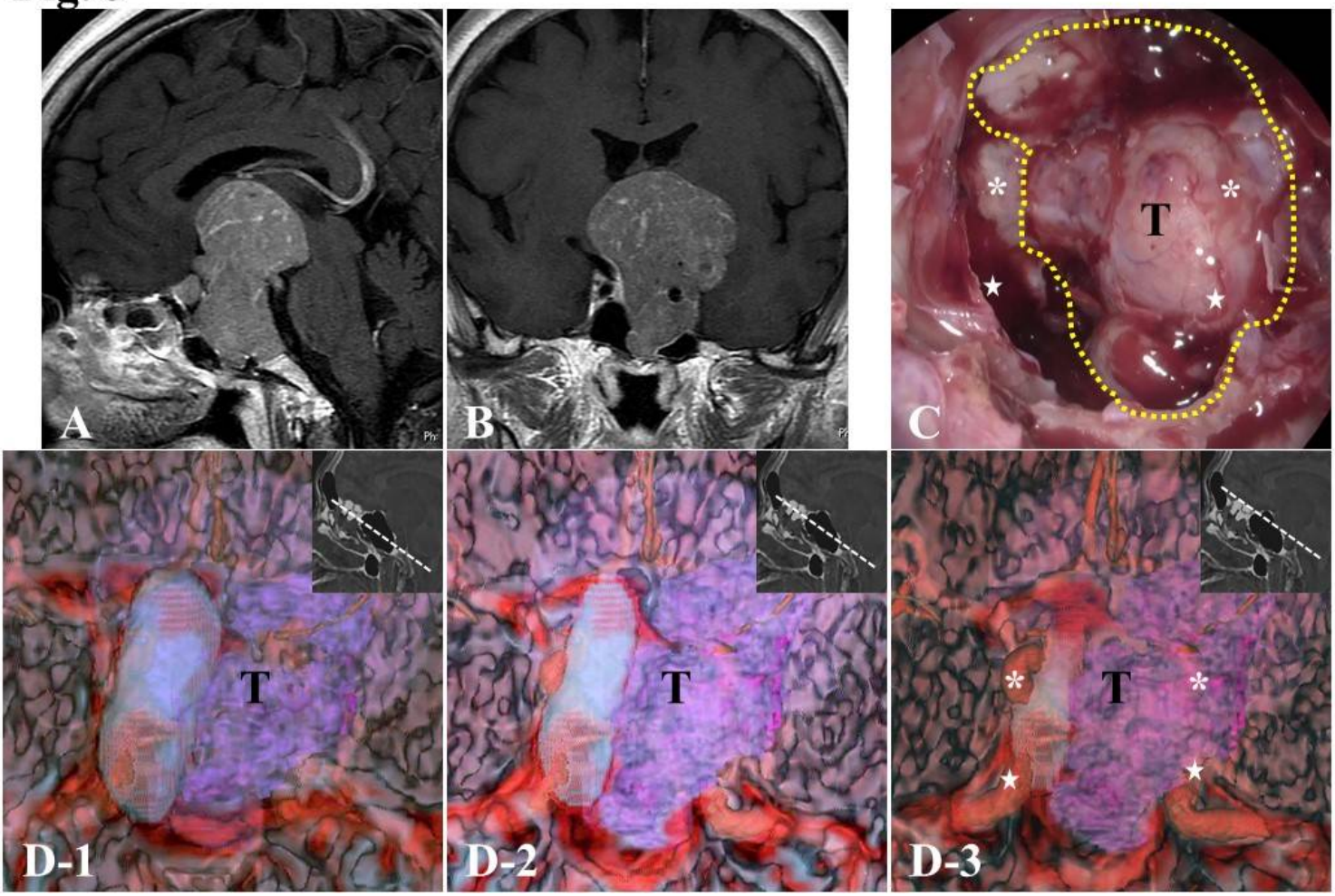

Figure 5

Preoperative Gd-enhanced MRI (A: sagittal view; B: coronal view) and intraoperative endoscopic image (C) in Case 2 showing a pituitary tumor invading into the sphenoid sinus with suprasellar extension (T: tumor, inside area of yellow dashed circle). A 3D-ZTE-based MRI model demonstrates that left ICAs (C3: white asterisk; C4: white star) are buried in invasive tumor at the sphenoid sinus by successive elimination of tumor on MRI (D).

Supplementary Files

This is a list of supplementary files associated with this preprint. Click to download.

- Table1.pdf